Supporting Information

Synthesis and Crystallization-Driven Self-Assembly of Triblock Copolymers Based on Narrowly Distributed α,ω-Bifunctionalized Conjugated Polymers

Donglai Tian, Bin Huang, Huanghao Pan, Yanchen Deng, Guiyou Wang and Aiguo Hu**

Shanghai Key Laboratory of Advanced Polymeric Materials, School of Materials Science and Engineering, East China University of Science and Technology, Shanghai, 200237, China.

*Corresponding Authors: hagmhsn@ecust.edu.cn (AH) and guiyouwang@ecust.edu.cn (GW)

Contents

Materials

Unless otherwise noted, all reagents were purchased from commercial sources and used without further purification. N, N-dimethylacetamide (DMAc) and dichloromethane (DCM) were distilled over calcium hydride before use. 1,4-bis(hexyloxy)-2,5-diiodobenzene[1], 1,4-bis(2-ethylhexyloxy)-2,5-diiodobenzene[2], 2,6-bis(trimethyltin)-4,8-di(2-ethylhexyloxy) benzo[1,2-b:4,5-b']dithiophene[3], 2,6-bis(trimethylstannyl)benzo[1,2-b:4,5-b']dithiophene[4] and SBA-15[5, 6] were synthesized according to literature procedures.

Characterizations and Measurements

Gel Permeation Chromatography (GPC). Number-averaged molecular weight (M_n) and dispersity ($Đ$) were measured by a gel permeation chromatography (GPC) system, which equipped with a Waters 1515 isocratic HPLC pump and a Waters 2414 refractive index detector. Narrowly distributed polystyrene (PS) was chosen as the standard. THF was chosen as the eluent (1 mL/min, 40 ℃) for the measurement of all samples.

Nuclear Magnetic Resonance Spectroscopy (NMR). ^{1}H NMR spectra were obtained from a Bruker AVANCE FT NMR spectrometer in $CDCl_3$ equipped with a TXIZ probe head (600 MHz) or a Bruker AVANCE FT NMR spectrometer in $CDCl_3$ equipped with Broadband high resolution probe head (400 MHz).

High-Resolution Transmission Electron Microscopy (HR-TEM). The HR-TEM images were recorded through a JEM-2100 microscope (JEOL, Japan) at an acceleration voltage of 200 kV. TEM samples were prepared by dropping 4 μL of the micellar solution onto carbon-coated copper grids; then, the samples were negatively stained with phosphotungstic

acid (PTA) aqueous solution. Images were analyzed with the software Image J (NIH). For the statistical analyses, more than N = 100 micelles in several images were traced by the software to obtain the length or width information. The number average micelle length/width (L_n/W_n) and weight average micelle length/width (L_w/W_w) (for the 1D cylindrical micelles) were calculated as shown below.

$$L_{\mathrm{n}} = \frac{\sum_{i=1}^{n} N_i L_i}{\sum_{i=1}^{n} N_i},\ L_{\mathrm{w}} = \frac{\sum_{i=1}^{n} N_i L_i^2}{\sum_{i=1}^{n} N_i L_i} \tag{1}$$

The width of the micelles was determined using a similar method, more than 200 micelles or positions in several images were traced by the software. The number average micelle width (W_n) and weight average micelle width (W_w) were calculated as shown below.

$$W_{\mathrm{n}} = \frac{\sum_{i=1}^{n} N_i W_i}{\sum_{i=1}^{n} N_i},\ W_{\mathrm{w}} = \frac{\sum_{i=1}^{n} N_i W_i^2}{\sum_{i=1}^{n} N_i W_i} \tag{2}$$

Nitrogen Adsorption/Desorption Isotherms. The isotherms were recorded by an adsorption apparatus on an ASAP2010 instrument. The surface area of Pd@SBA-15 was calculated from the Brunauer–Emmett–Teller (BET) equation. The pore size distribution was calculated from the desorption branch of the isotherms by means of the Barrett-Joyner-Halanda (BJH) approach.

Inductively Coupled Plasma Atomic Emission Spectroscopy. The sample of Pd@SBA-15 was digested in aqua regia at 100 ℃. The palladium content of Pd@SBA-15 was measured by an Agilent 725 ICP-AES instrument.

Fluorescence emission spectra were obtained on Lumina (Thermo fisher, USA) at 25 ˚C in DCM and aqueous solution (1 μg/mL, λ_{ex} = 365 nm).

UV-vis spectra were recorded by an Evolution 201 UV spectrophotometer (Thermo fisher, USA) at 25 ˚C in either DCM or aqueous solution (1 μg /mL).

Laser Scanning Confocal Microscopy (LSCM). Confocal imaging was performed using a Leica stellaris5 system attached to a Leica DMl6000 inverted epifluorescence microscope with a100x (NA 1.4) oil immersion objective lens. 10 μL of the sample solution was applied to a microscope slide. The sample were excited using a UV diode laser operating at 405 nm. Confocal images were obtained using digital detectors with observation windows of 410-500 nm. Micelle concentrations of ca.1 mg/mL in aqueous solution were used for imaging experiments.

Differential scanning calorimetry (DSC). Thermal properties of the samples were measured on a DSC 2910 (TA Instruments). Samples (5 mg) were put into aluminum pans and heated from room temperature to 120 °C or 250 °C at a rate of 10 °C/min under N_2 atmosphere with a flow rate of 40 mL/min, respectively. The samples were held at that temperature for 2 min to erase any thermal history, then were cooled to room temperature at a rate of 10 °C/min. After that, samples were reheated again at a rate of 10 °C/min under N_2 atmosphere with a flow rate of 40 mL/min.

Thermogravimetric analysis. TGA/DTG measurements were conducted using a Netzsch TG 209F3, with 5-10 mg samples placed in open alumina crucibles. The samples were heated at a rate of 10 K min^{-1} under a nitrogen atmosphere. The temperature range was from 30 to 800 °C, with a gas flow rate of 60 mL min^{-1}.

Density functional theory (DFT). DFT studies have been carried out with Gaussian 09 program53 using the B3LYP exchange and correlation functional and the 6-31G(d,p) basis set in gas phase.

Dynamic Light Scattering (DLS). The hydrodynamic diameters of CP_1-$MPEG_{45}$ were measured in THF and H_2O dispersions (1 mg/mL) using a Zetasizer Nano ZS (Malvern, UK) at 25 °C, with a 633 nm laser and 173° backscatter angle.

Synthesis of Monomers

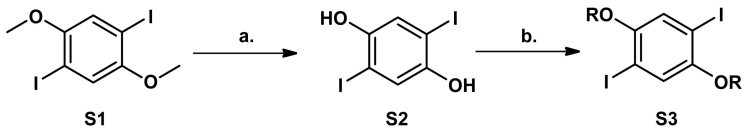

S1 S2 S3

a. BBr_3, DCM, -78°C
b. KOH, RBr, DMSO, R.T.

S3-1: R=2-ethylhexyl
S3-2: R=n-hexyl

S2[2]**:** 1,4-diiodo-2,5-dimethoxybenzene (**S1**, 8.0 g, 0.020 mol) placed into a 250 mL Schlenk flask, which was evacuated and purged with argon three times. Anhydrous DCM (100 mL) was then added, and the flask was immersed in a dry ice/acetone bath. After stirring for 15 min, BBr_3in DCM (1.0 M, 80 mL, 0.080 mol) was added via syringe. The solution was allowed to return to room temperature and stirred for 16 h. The reaction mixture was then poured into ice water, resulted in a white precipitate. The mixture was filtered, washed with dichloromethane three times, and vacuum-dried to remove residual solvent, yielding the product as a white powder (6.75 g, 91%).

S3-1[1]: **S2** (6.75 g, 18.65 mmol) and KOH (4.71 g, 83.93 mmol) were added to a 100 mL round-bottom flask containing anhydrous DMSO (30 mL). The reaction mixture was stirred at room temperature under a nitrogen atmosphere for 1 h. Using a syringe, 2-ethylhexyl

bromide (7.92 g, 41.03 mmol) was added, and the reaction continued for 24 h. The reaction mixture was then poured into saturated brine (200 mL) and extracted with DCM (100 mL) for three times. The DCM phase was collected and the solvent was removed. The crude product was dissolved in ethyl acetate (150 mL), and the organic phase was washed with deionized water three times. After removal of solvent, the crude product was purified by silica gel column chromatography with hexane as eluent to get **S3-1** (7.89 g, 72%) as a colorless oil. ^{1}H NMR (400 MHz, $CDCl_3$) δ: 7.16 (s, 2H) 3.81 (d, J = 5.5 Hz, 4H) 1.73 (m, 2H) 1.61-1.29 (m, 16H) 0.99 - 0.83(m, 12H).

S3-2: The brominating reagent used was 1-bromohexane (6.77 g, 41.03 mmol). The synthesis route was identical to that for **S3-1**, yielding a white powder, **S3-2** (8.35 g, 84%).^{1}H NMR (400 MHz, $CDCl_3$) δ: 7.17 (s, 2H), 3.92 (t, J = 6.4 Hz, 4H), 1.84 – 1.74 (m, 4H), 1.54 – 1.43 (m, 4H), 1.38 -1.33 (m, 8H), 0.91 (t, J = 6.8 Hz, 6H).

Synthesis of MPEG-I

General procedure for the synthesis of MPEG-I[7]:

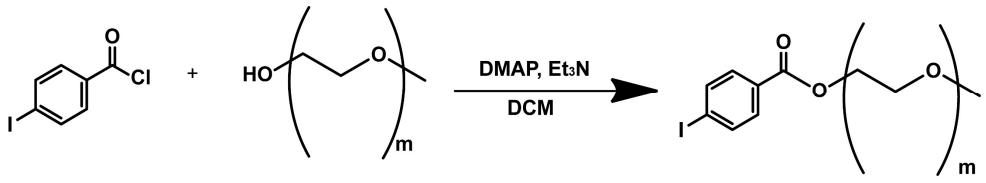

Methoxy polyethylene glycols (MPEG, 1 equiv.), 4-iodobenzoyl chloride (3 equiv.), triethylamine (3 equiv.), and DMAP (0.1 equiv.) were stirred at room temperature in dry DCM under a nitrogen atmosphere for 24 h. The product was filtered, and the filtrate was washed with saturated sodium carbonate solution and 1 M HCl. The organic layer was concentrated by rotary evaporation. The residue was precipitated using hexane as a poor

solvent and DCM as a good solvent, yielding MPEG-I. ^{1}H NMR (600 MHz, $CDCl_3$): δ (ppm) 7.82 – 7.68 (m, Ar–H), 3.68–3.57 (m, $–CH_2CH_2–$).

$MPEG_{12}$-I: A colorless, oil-like liquid $MPEG_{12}$-I (2.91 g, 74.6%) was prepared using MPEG ($M_{n,\ NMR}$ = 550 g mol^{-1}, 2.75 g, 5 mmol).

$MPEG_{22}$-I: A white powder, $MPEG_{22}$-I (5.37 g, 87.3%), was prepared using MPEG ($M_{n,\ NMR}$ = 1000 g mol^{-1}, 5 g, 5 mmol).

$MPEG_{45}$-I: A white powder, $MPEG_{45}$-I (10.89 g, 97.7%), was prepared using MPEG ($M_{n,\ NMR}$ = 2000 g mol^{-1}, 10 g, 5 mmol).

$MPEG_{113}$-I: A white powder, $MPEG_{45}$-I (10.43 g, 99.7%), was prepared using MPEG ($M_{n,\ NMR}$ = 5000 g mol^{-1}, 10 g, 2 mmol).

Synthesis of Pd@SBA15[8-10]

SBA-15: A 500 mL round-bottom flask was charged with P123 (EO_{20}-PO_{70}-EO_{20}, M_n = 5800, 5.0 g), which was dissolved in deionized water (319 mL) and concentrated hydrochloric acid (53 mL). The solution was stirred slowly at 40 °C until clear. Tetraethyl orthosilicate (22.2 mL) was then added dropwise, causing the solution to gradually turn white. The mixture was stirred for an additional 20 h, then transferred to a PTFE-lined container. This container was placed in a stainless steel autoclave and subjected to crystallization at 100 °C for 20 h. After cooling to room temperature, the mixture was filtered. The resulting solid was washed with deionized water and ethanol, and then dried under vacuum at 60 °C to obtain white powder, SBA-15 (10.0 g).

Re-SBA-15: In a 250 mL round-bottom flask, SBA-15 (10.0 g) and P123 (40.0 g) were added, followed by absolute ethanol (150 mL). The mixture was stirred at room temperature for 24 hours. The product was then filtered, and the resulting white powder was dried under vacuum at 60 °C to obtain Re-SBA-15.

HMDS-Re-SBA-15: Re-SBA-15 (10.0 g) and hexamethyldisilazane (125 mL) were added to a 250 mL round-bottom flask and stirred at room temperature for 3 h. The mixture was filtered, washed with n-hexane, and then dried under vacuum at 60 °C to obtain HMDS-Re-SBA-15.

EX-HMDS-Re-SBA-15: The HMDS-Re-SBA-15 was Soxhlet-extracted with ethanol for 7 days, and then dried under vacuum at 60 °C to obtain EX-HMDS-Re-SBA-15.

SBA-15-NH_2: EX-HMDS-Re-SBA-15 (4.0 g) was placed in a 250 mL round-bottom flask, to which anhydrous toluene (50 mL) and 3-aminopropyltriethoxysilane (APTES, 13.34 mL) were added. The mixture was refluxed under nitrogen atmosphere for 48 h. Subsequently, it was washed three times with acetone and chloroform, and then dried in a vacuum oven at 60 °C to give SBA-15-NH_2.

Pd@SBA-15: SBA-15-NH_2 (1.0 g) was placed in a 250 mL flask, to which DMF (100 mL) was added, and the mixture was sonicated for 15 min. At room temperature, the mixture was stirred vigorously for 10 min while a solution of H_2PdCl_4 (10 mM, 6 mL) was added dropwise. After sonication for 15 min, the mixture was stirred for 4 h. A freshly prepared $NaBH_4$ solution (1 M, 5 mL) was then added dropwise to the solution, and stirring continued for an additional 12 h. The product was filtered, washed three times each with deionized

water and ethanol, and then dried in a vacuum oven at 60 °C to obtain Pd@SBA-15. The palladium content of Pd@SBA-15 is 0.6 wt%, with a pore size of 7 nm (**Figure S10**).

Synthesis of conjugated polymers and triblock copolymers

The NHC-Pd catalyst was synthesized according to the method described in the literature[11].

CP_1-Bpin: A mixture of 1,4-bis(2-ethylhexyloxy)-2,5-diiodobenzene (586.3 mg, 1 mmol), 1,4-benzenediboronic acid bis(pinacol) ester (330.0 mg, 1 mmol), Pd@SBA15 (177.4 mg, 0.01 mmol), Cs_2CO_3 (977.5 mg, 3 mmol) and N,N-dimethylacetamide (DMAc, 10 mL) was added to a 25 mL Schlenk flask. After three freeze-pump-thaw cycles, the tube was sealed under nitrogen atmosphere and stirred at 80 °C for 48 h. Subsequently, 1,4-benzenediboronic acid bis(pinacol) ester (165 mg, 0.5 mmol) and NHC-Pd (7 mg, 0.01 mmol) were added in situ, and the reaction was continued for 24 h. The product was washed with methanol and collected with filtration (335 mg, 82 %). **CP_2-Bpin** (248 mg, 70%), **CP_3-Bpin** (206 mg, 85%), **CP_4-TMT** (485 mg, 80%) and **CP_5-TMT** (313 mg, 60%) were obtained using a similar synthetic route.

$CP_{1\text{-}SGP}$-Bpin: The boronic ester monomer was used in slight excess to achieve a molecular weight roughly comparable to that of **CP_1-Bpin**. A mixture of 1,4-bis(2-ethylhexyloxy)-2,5-diiodobenzene (586.3 mg, 1 mmol), 1,4-benzenediboronic acid bis(pinacol) ester (379.5 mg, 1.15 mmol), NHC-Pd (7 mg, 0.01 mmol), Cs_2CO_3 (977.5 mg, 3 mmol) and N,N-dimethylacetamide (DMAc, 10 mL) was added to a 25 mL Schlenk flask. After three freeze-pump-thaw cycles, the tube was sealed under nitrogen atmosphere and stirred at 80 °C for 24 h. Subsequently, 1,4-benzenediboronic acid bis(pinacol) ester (165 mg,

0.5 mmol) was added in situ, and the reaction was continued for 24 h. The product was washed with methanol and collected with filtration (342 mg, 84 %).

CP_1-$MPEG_{12}$: A mixture of CP_1-Bpin (50 mg, 0.0125 mmol), $MPEG_{12}$-I (41.3 mg, 0.075 mmol), NHC-Pd (3 mg, 0.004 mmol), Cs_2CO_3 (100 mg, 0.3 mmol) and N,N-dimethylacetamide (DMAc, 2 mL) was added to a 10 mL Schlenk flask. After three freeze-pump-thaw cycles, the tube was sealed under nitrogen atmosphere and stirred at 80°C for 2 h. After cooling the reaction mixture to room temperature, deionized water was added, and the solution was centrifuged to collect the filtrate. This process was repeated several times to remove residual polymer. The filtrate was then transferred to an appropriate dialysis bag and dialyzed to remove inorganic salts and excess $MPEG_m$-I. The final product was obtained by freeze-drying. **CP_n-$MPEG_m$** were prepared sequentially following a similar synthetic route. All of the triblock copolymers were obtained with a high yield (> 90%).

Preparation of the Micellar Solutions

CP_1-$MPEG_{22}$ (25 mg) was dissolved in THF (1 mL), and deionized water (10 mL) was added dropwise to the solution. THF was then removed using dialysis against deionized water. The micellar solution was transferred to a volumetric flask and the dialysis bag was rinsed repeatedly with deionized water and collected to the volumetric flask. The final volume of the micellar solution was adjusted to 25.0 mL by addition of deionized water, achieving a micellar solution concentration of 1 mg/mL. The micellar solutions of **CP_n-$MPEG_m$** were prepared using a similar procedure.

Thermodynamic property testing

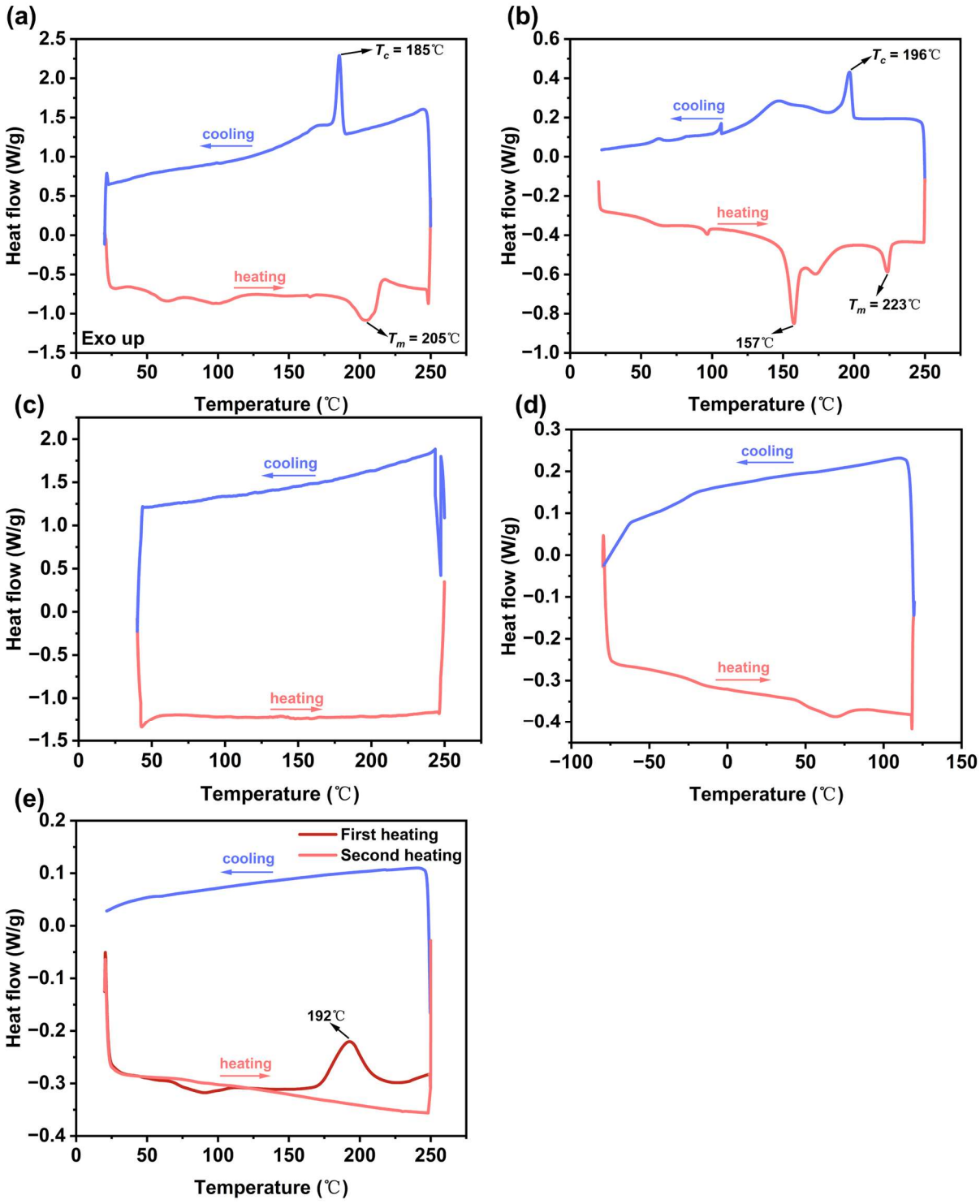

Figure S1. DSC curves of CP_1 (a), CP_2 (b), CP_3 (c), CP_4 (d) and CP_5 (e).

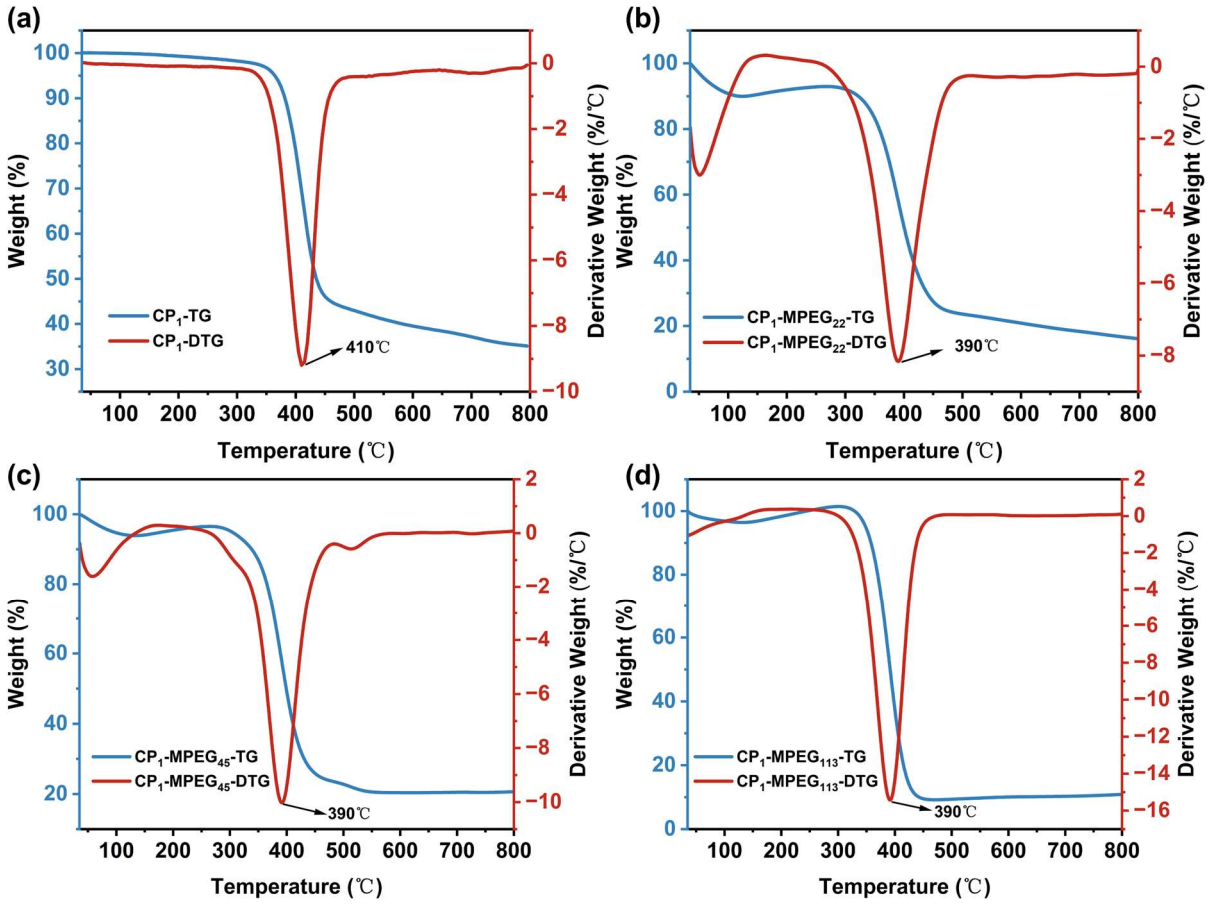

Figure S2. TGA and DTG curves of CP_1 (a), CP_1-$MPEG_{22}$ (b), CP_1-MPE45 (c) and CP_1-$MPEG_{113}$ (d).

GPC measurement

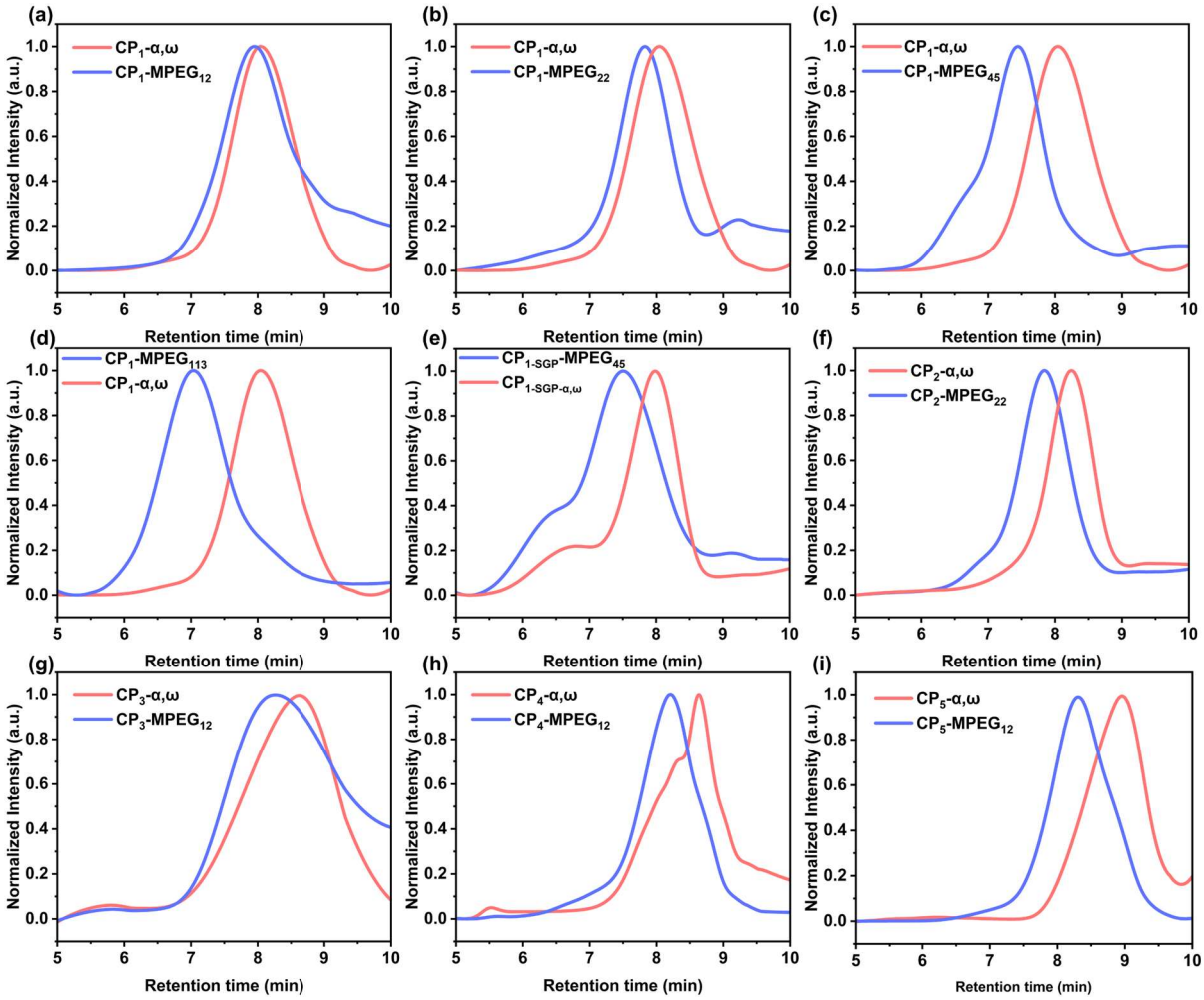

Figure S3. The GPC profiles of conjugated polymers and triblock copolymers.

The characterization of micelles

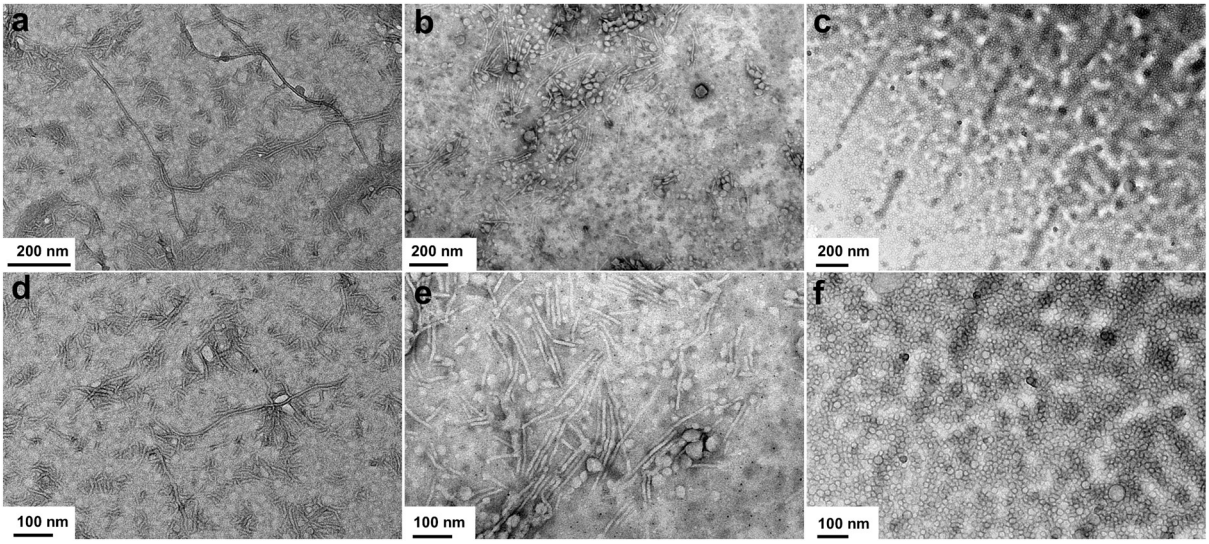

Figure S4. TEM images of the micelles of triblock copolymers dispersed in water (1 mg/mL): CP_2-$MPEG_{22}$ (a) and (d); $CP_{1\text{-}SGP}$-$MPEG_{45}$ (b) and (e); CP_3-$MPEG_{12}$ (c) and (f). For CP_2-$MPEG_{22}$, shown in (a) and (d): L_n = 114 nm, L_w/L_n =1.42; W_n = 8.51 nm, W_w/W_n =1.02.

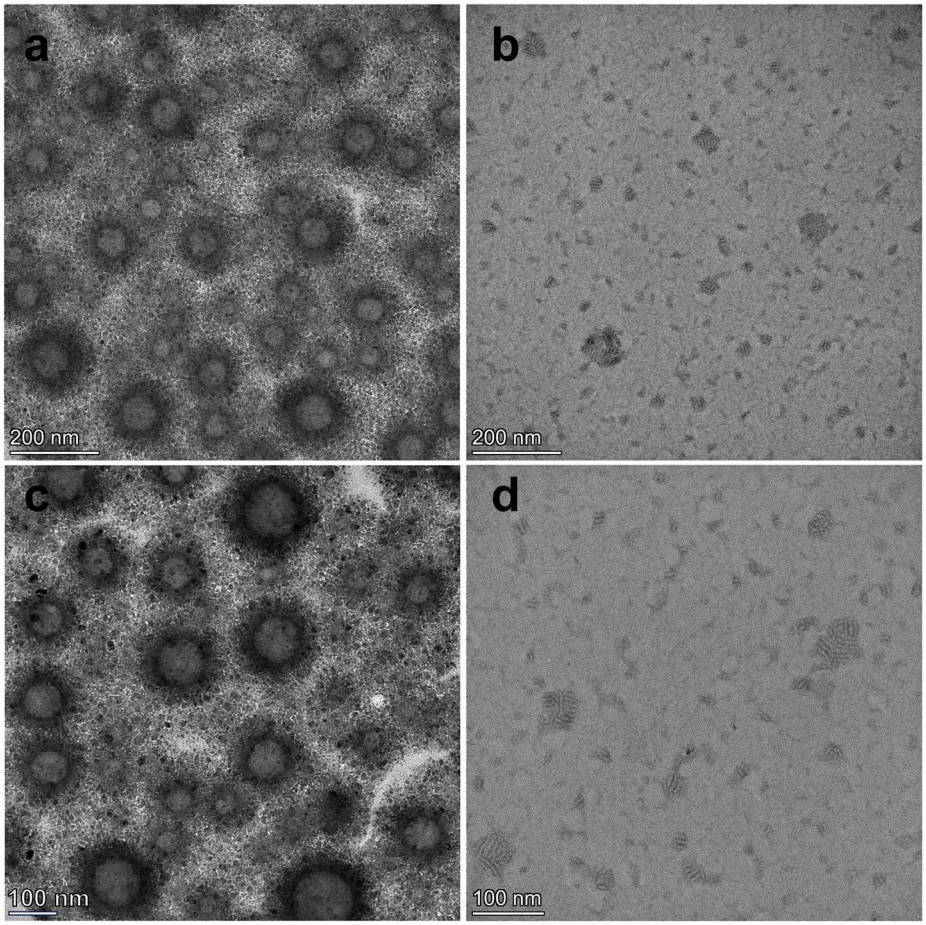

Figure S5. TEM images of the micelles of triblock copolymers dispersed in water (1 mg/mL): CP_4-$MPEG_{12}$ (a) and (c); CP_5-$MPEG_{12}$ (b) and (d). For CP_5-$MPEG_{12}$, shown in (b) and (d): L_n = 25 nm, L_w/L_n =1.19; W_n = 4.00 nm, W_w/W_n =1.03.

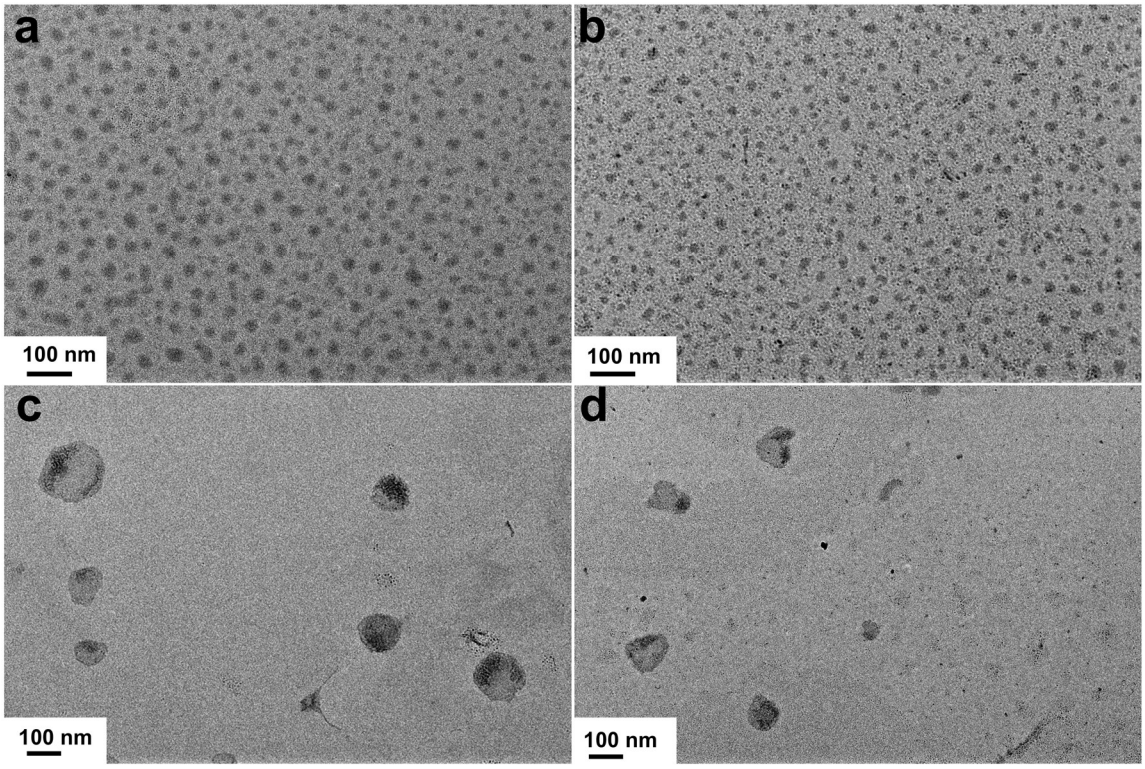

Figure S6. TEM images of phosphotungstic acid aqueous solution (a,c) and CP_1-$MPEG_{45}$ dispersed in THF (b,d) at a concentration of 1 mg/mL.

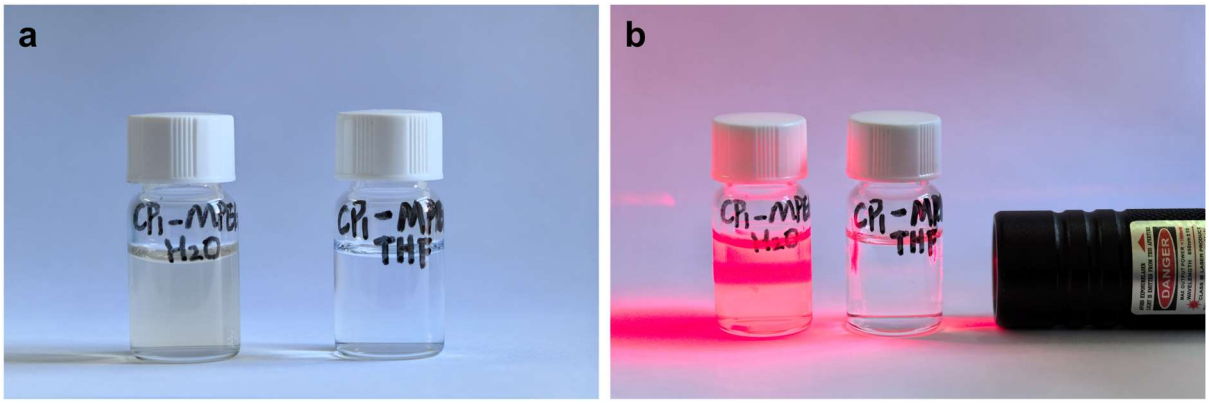

Figure S7. Optical images of CP_1-$MPEG_{45}$ aqueous solution and CP_1-$MPEG_{45}$ THF solution at a concentration of 1 mg/mL under natural light (a), and laser irradiation images (b).

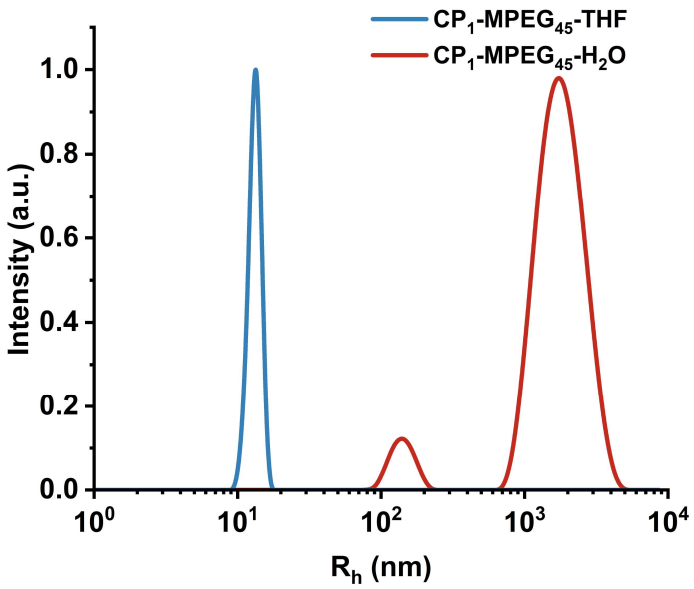

Figure S8. Hydrodynamic radius of the CP_1-$MPEG_{45}$ in THF and H_2O dispersion at 25 °C.

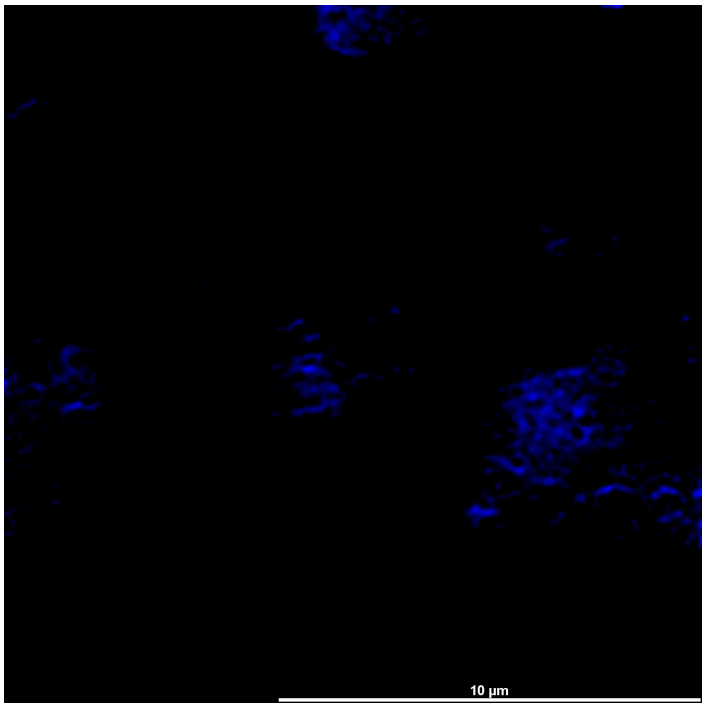

Figure S9. Laser confocal microscopy images of CP_1-$MPEG_{45}$ in aqueous solution.

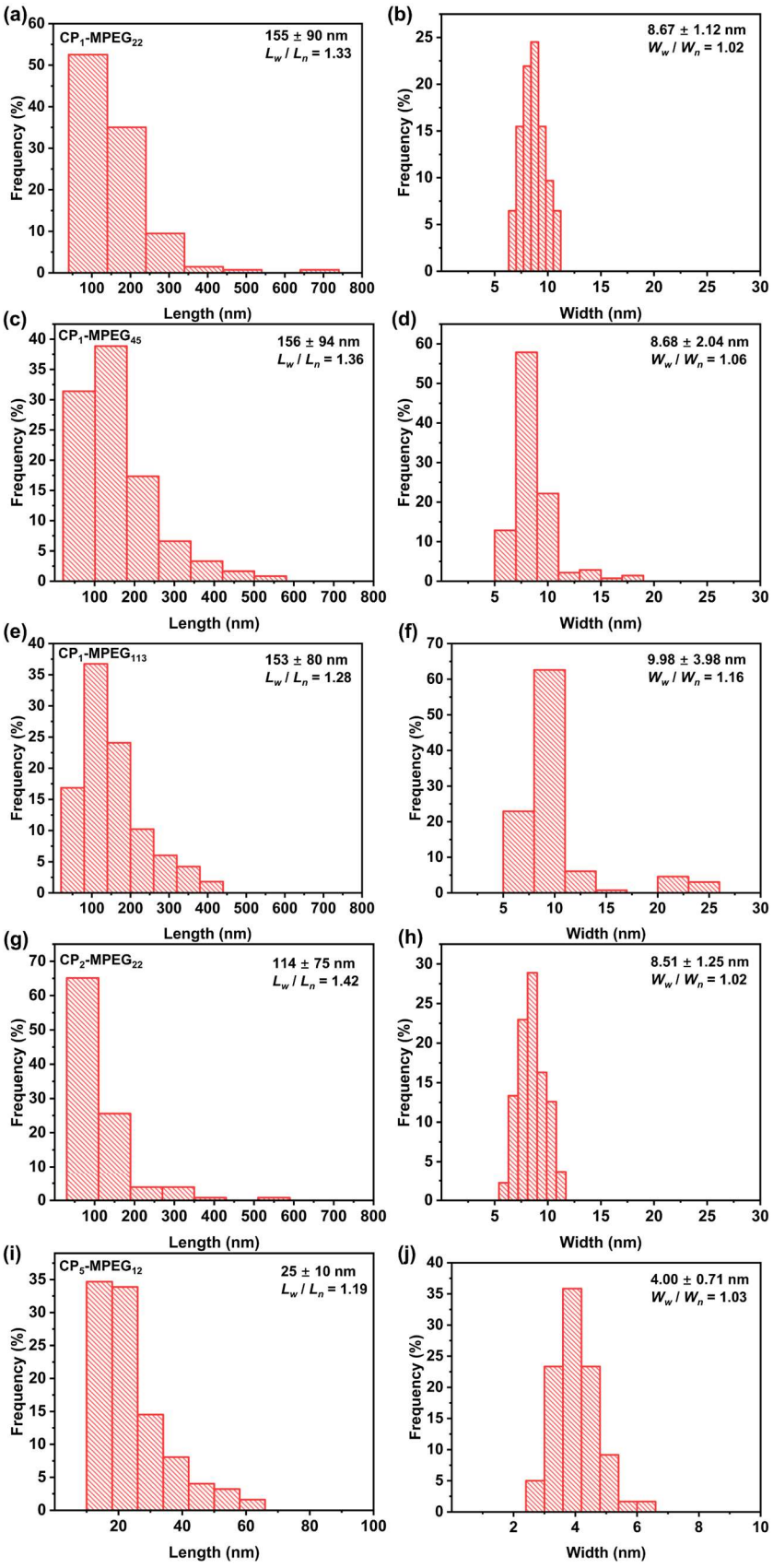

Figure S10. Histogram of the length and width distribution of the rod-like micelles analyzed from TEM images.

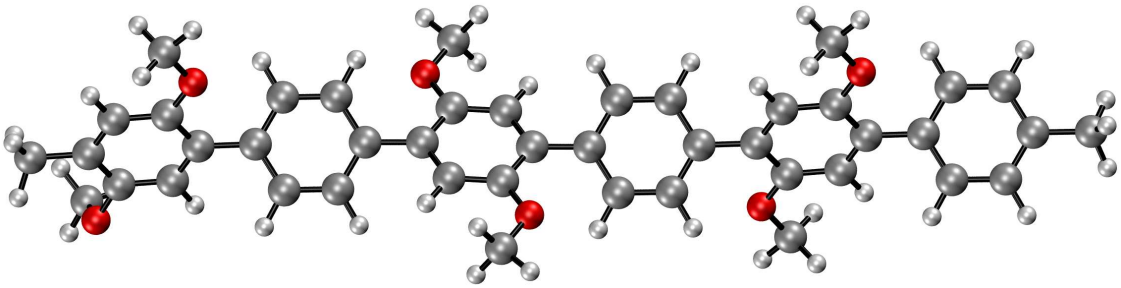

Figure S11. The structure optimization diagram of the CP_1 or CP_2 (3 repeating units) determined from B3LYP/6.31G(d,p) calculations.

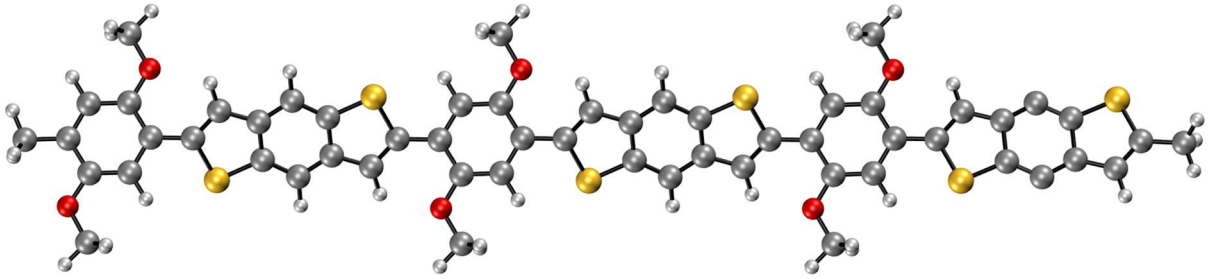

Figure S12. The structure optimization diagram of the CP_5 (3 repeating units) determined from B3LYP/6.31G(d,p) calculations.

Absorption and fluorescence emission spectra measurements

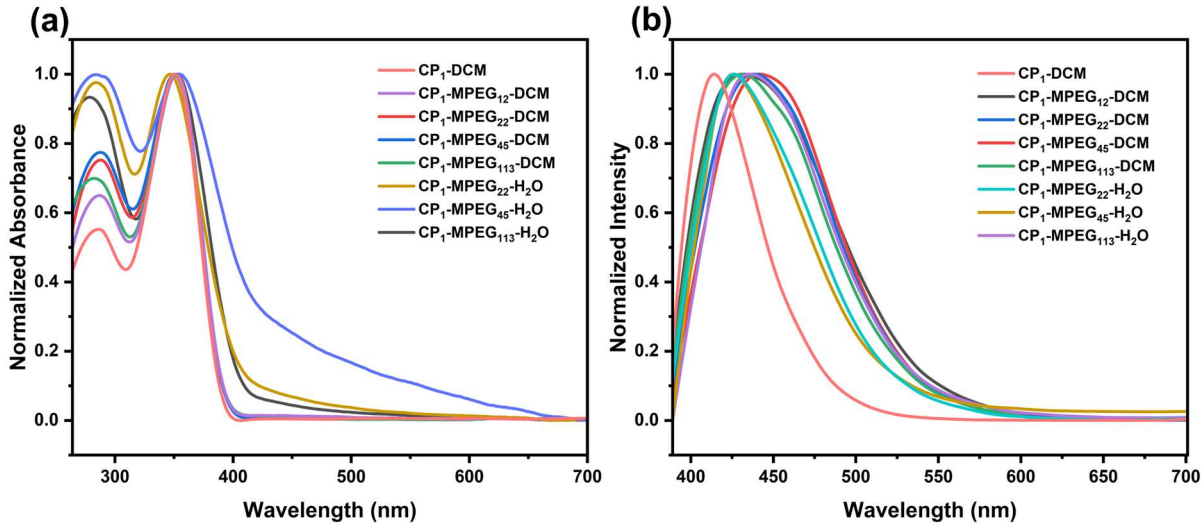

Figure S13. UV-vis absorption spectra (a, 1 μg/mL) and fluorescence emission spectra (b, 1 μg/mL, λ_{ex} = 365 nm) of **CP1** and its derivatives.

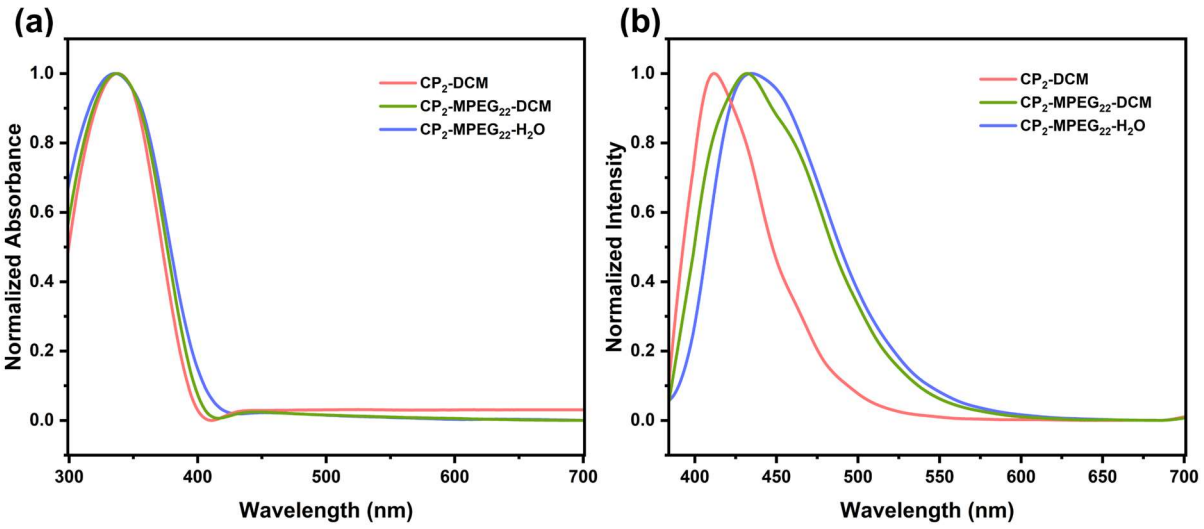

Figure S14. UV-vis absorption spectra (a, 1 μg/mL) and fluorescence emission spectra (b, 1 μg/mL, λ_{ex} = 365 nm) of **CP2** and its derivatives.

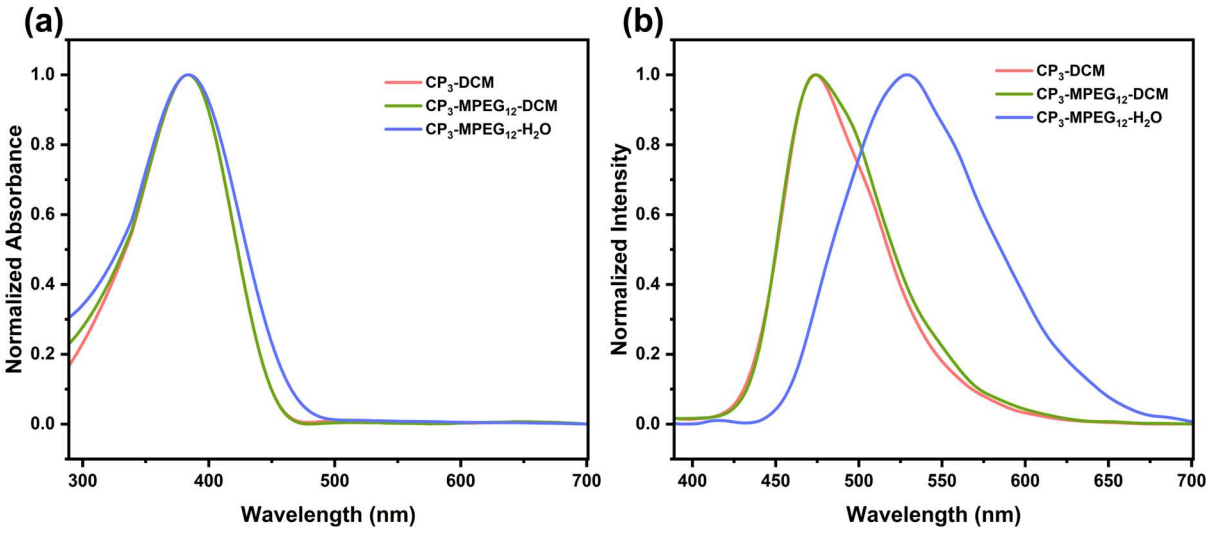

Figure S15. UV-vis absorption spectra (a, 1 μg/mL) and fluorescence emission spectra (b, 1 μg/mL, λ_{ex} = 365 nm) of **CP3** and its derivatives.

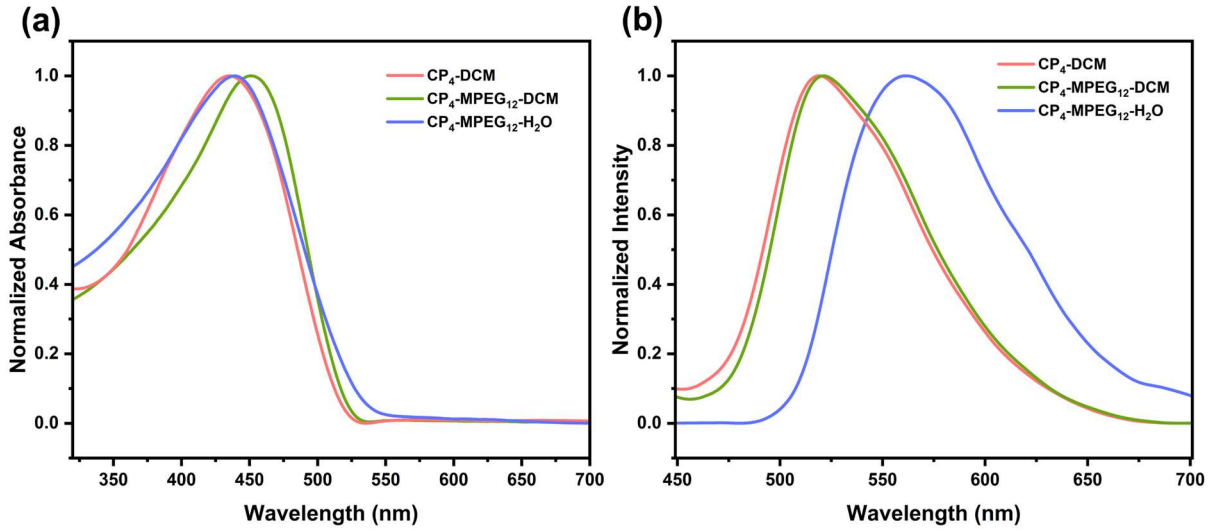

Figure S16. UV-vis absorption spectra (a, 1 μg/mL) and fluorescence emission spectra (b, 1 μg/mL, λ_{ex} = 365 nm) of **CP4** and its derivatives.

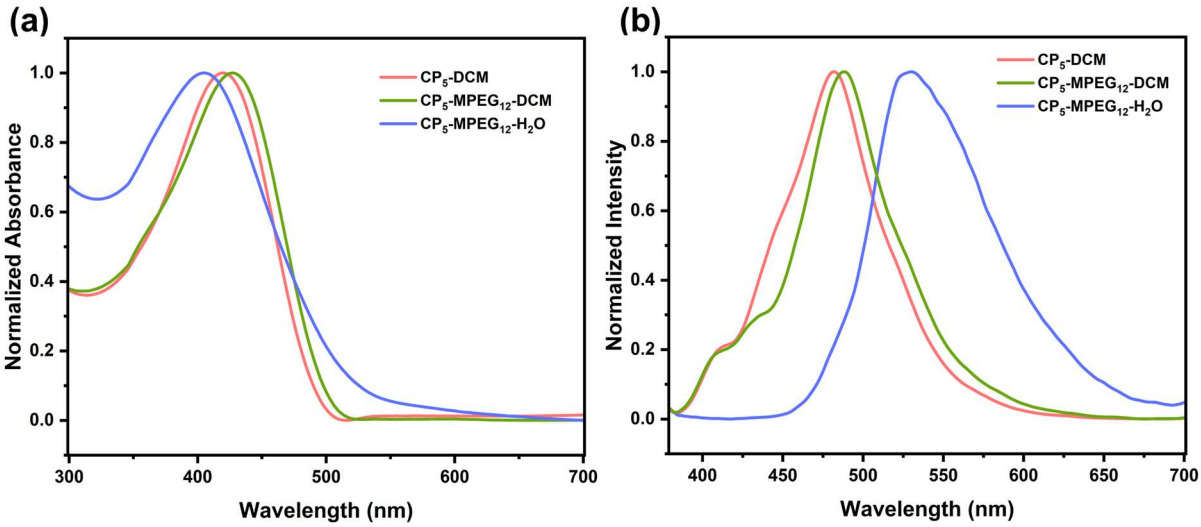

Figure S17. UV-vis absorption spectra (a, 1 μg/mL) and fluorescence emission spectra (b, 1 μg/mL, λ_{ex} = 365 nm) of **CP5** and its derivatives.

BET tests for the nanoreactors

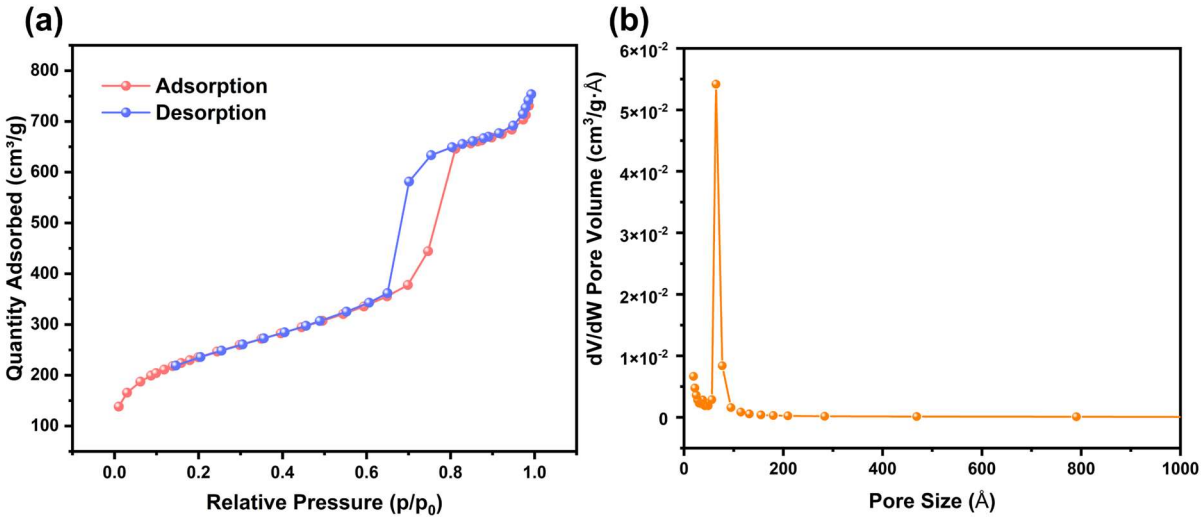

Figure S18. The N_2 adsorption and desorption curves (a) and the pore size distribution curve (b) of Pd@SBA-15.

^{1}H NMR analysis and discussion

The ^{1}H NMR spectra of these (end-functionalized) conjugated (block) polymers exhibit notable similarities (**Figure S19-S26**). Taking the ^{1}H NMR analysis of CP_1 and its derivatives as an example, the multiplets near 7.70 ppm (**Figure S19,** peaks b/d/e) and 7.10 ppm (**Figure S19,** peaks c/c*) are attributed to the aromatic protons present in the internal repeating units. The signal at 7.16 ppm (**Figure S19,** peak f) is associated with the protons located at the ortho positions of the iodine-terminated end groups, with additional contributions from the aromatic protons of residual monomer 1. The peak at 7.81 ppm indicates the presence of residual monomer 2. The multiplet at 7.89 ppm (**Figure S19,** peak a) corresponds to the protons of the benzene ring with terminal pinacol boronate groups. A comparative analysis of the ^{1}H NMR spectra for CP_1 and $CP_{1\text{-}\alpha,\omega}$ reveals the absence of the peak at 7.16 ppm, which signifies the complete end-capping of the polymer with phenylboronic acid pinacol ester. Following the reaction with $MPEG_m$-I, the disappearance of the signal at 7.89 ppm indicates the complete grafting of the hydrophilic chain segments. As shown in **Figure S21**, the number of repeat units (N=10) in the main chain of the conjugated polymer can be obtained by calculating the ratio of the integrated areas of the ^{1}H NMR peaks at 7.70 ppm and 7.89 ppm, which is in complete agreement with the result obtained from GPC analysis. Similarly, using the same method, the number of repeat units for $CP_{2\text{-}\alpha,\omega}$ (**Figure S22**, N=10) and $CP_{3\text{-}\alpha,\omega}$ (**Figure S23**, N=10) can be calculated, whereas the N obtained from GPC for $CP_{2\text{-}\alpha,\omega}$ and $CP_{3\text{-}\alpha,\omega}$ are 11, demonstrating the effectiveness of GPC in determining the molecular weight of conjugated polymers with rigid main chain structures. However, the more complex structures for $CP_{4\text{-}\alpha,\omega}$ and $CP_{5\text{-}\alpha,\omega}$ lead to excessive overlap of the peaks in the aromatic region,

making it impossible to assess the molecular weight via ^{1}H NMR. Nevertheless, due to the conjugated rigid structure of their main chain, the calculation of the degree of polymerization using GPC remains highly relevant for reference.

In the ^{1}H NMR spectra of CP_1-$MPEG_m$ (**Figure S20**, where m = 12, 22, 45, 113), the sharp peak at 3.63 ppm corresponds to the methylene groups within the MPEG segment while the broad peak at 3.85 ppm arises from the phenoxymethylene groups in the conjugated segment. Interestingly, the integration ratio of these two peaks increases linearly with the length of the MPEG segments (**Figure S22**), suggesting a consistent grafting reaction. For each specific block copolymer, the integration of these two peaks reflects an approximate 2:1 ratio of MPEG to conjugated blocks, thereby corroborating the successful synthesis of the amphiphilic triblock copolymers.

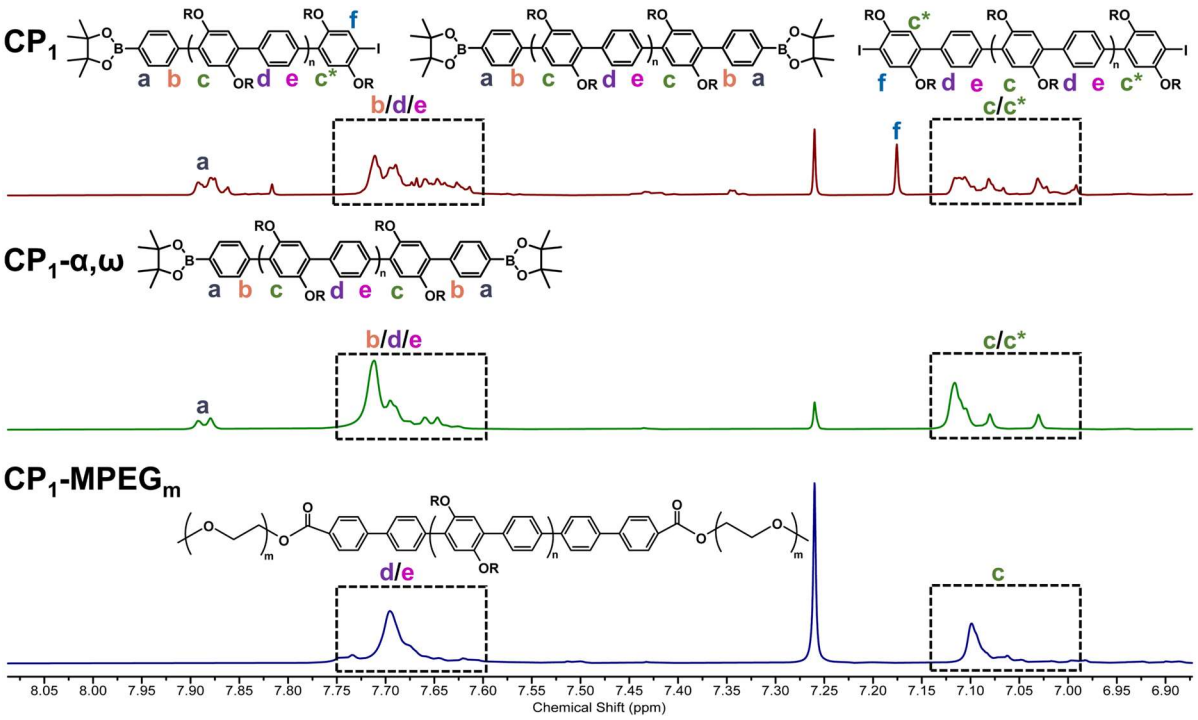

Figure S19. Aromatic regions of the ^{1}H NMR spectra of CP_1, $CP_{1\text{-}\alpha,\omega}$ and CP1-$MPEG_m$ (m = 45) in $CDCl_3$.

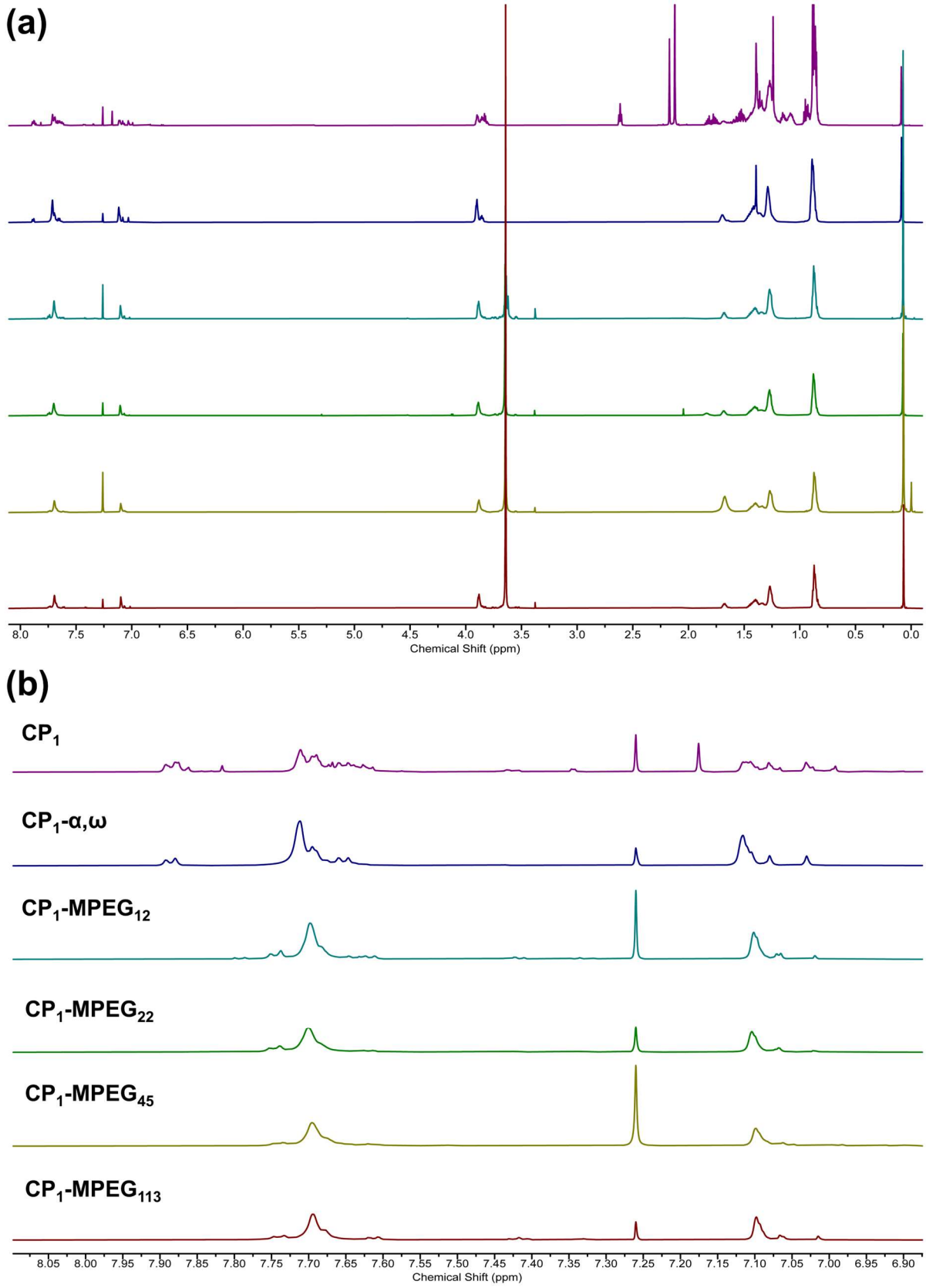

Figure S20. The ^{1}H NMR spectra of CP_1 and its derivatives in $CDCl_3$.

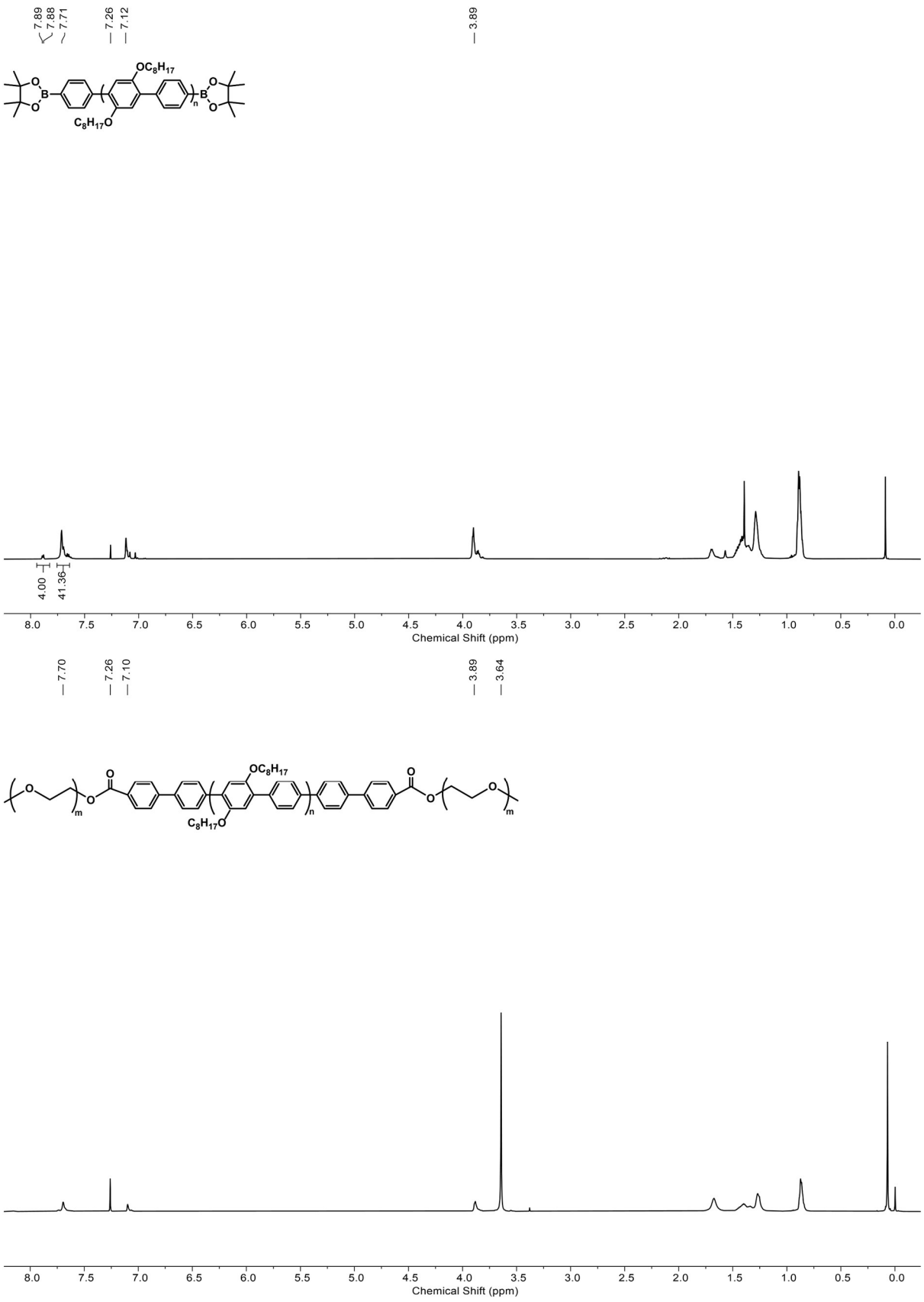

Figure S21. The ^{1}H NMR spectra of CP_1 and CP_1-$MPEG_{45}$ in $CDCl_3$.

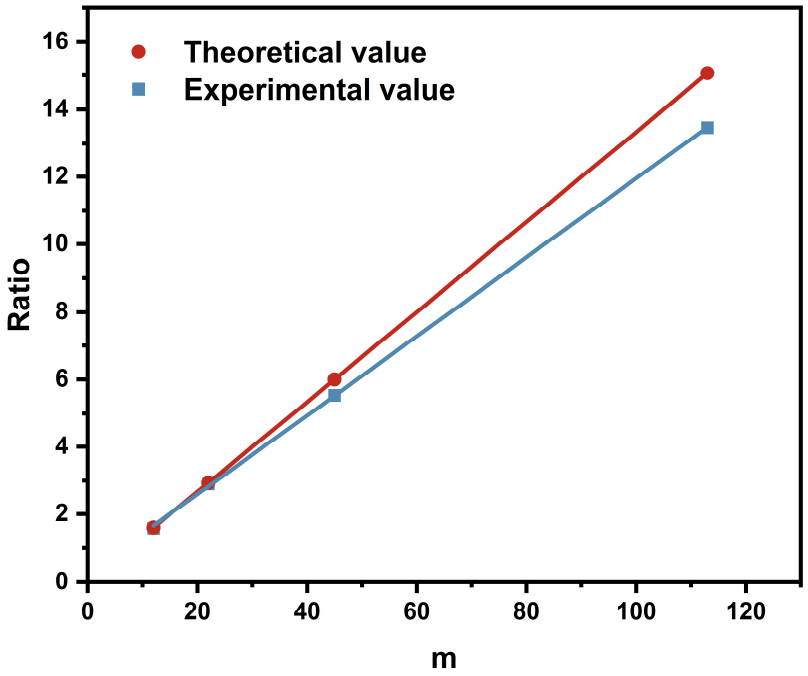

Figure S22. The ratio of the integral areas of the methylene and phenoxy-methylene groups in the MPEG segment of CP_1-$MPEG_m$ (m = 12, 22, 45, 113) from the ^1H NMR spectra.

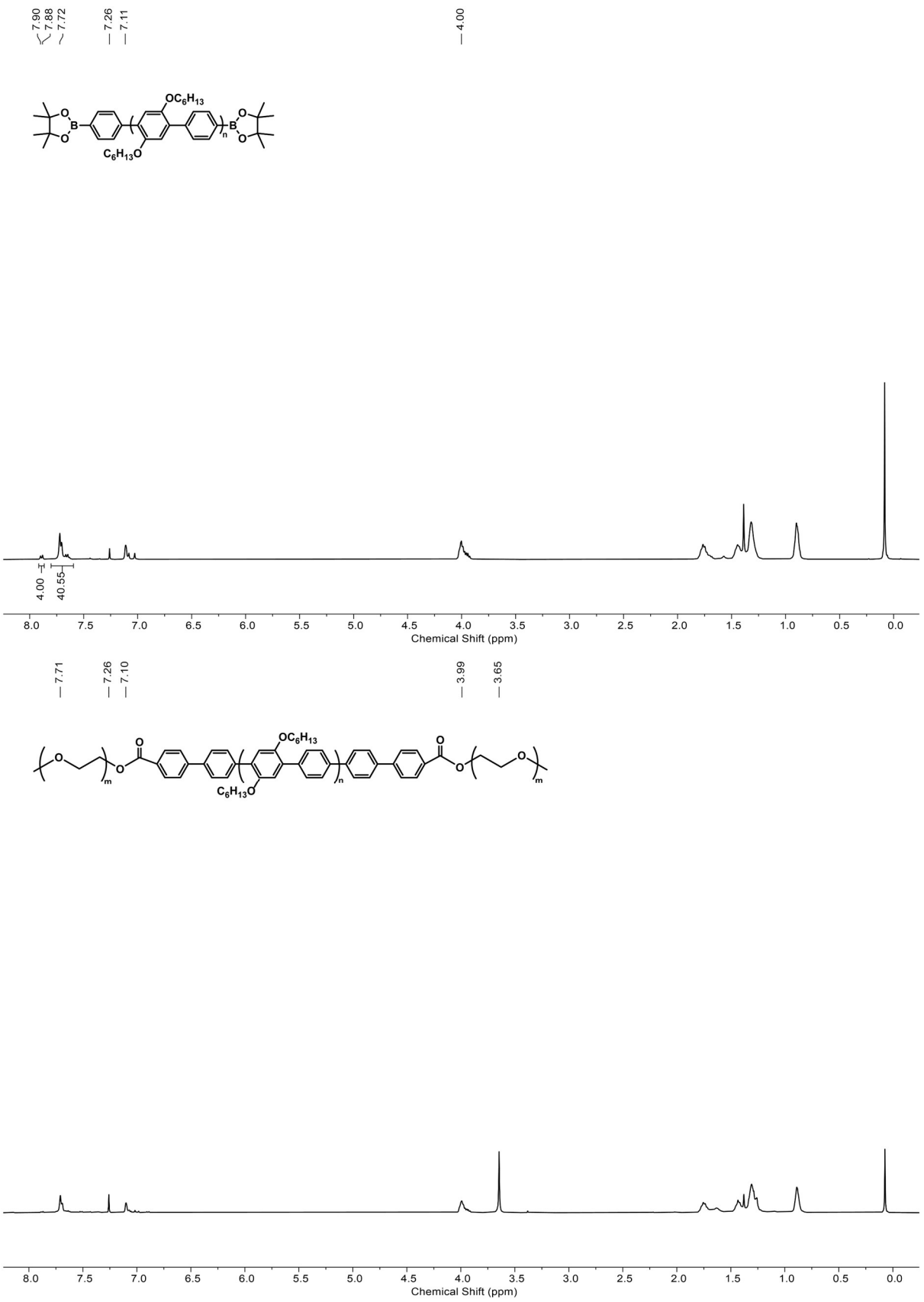

Figure S23. The ^{1}H NMR spectra of CP_2 and CP_2-$MPEG_{22}$ in $CDCl_3$.

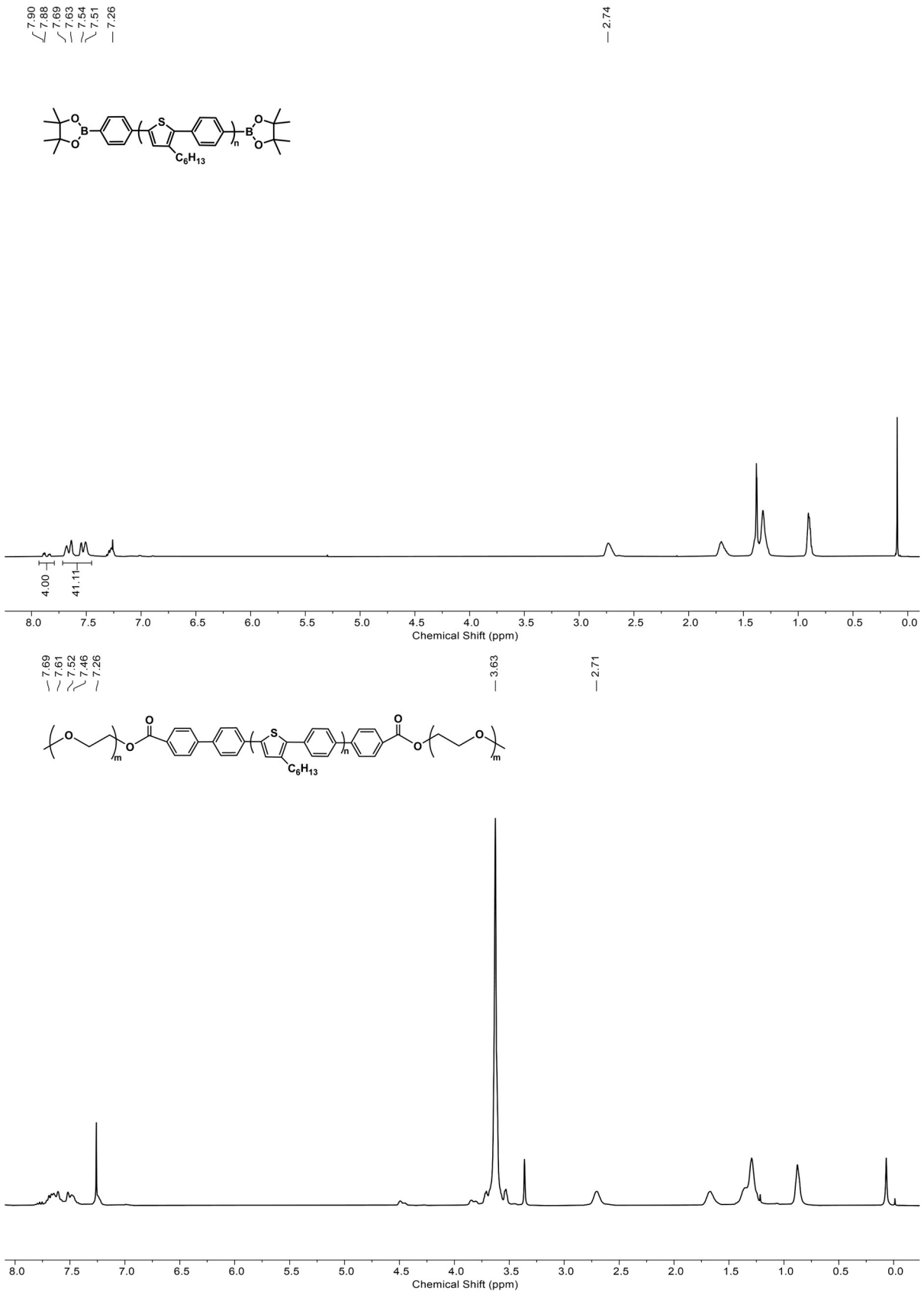

Figure S24. The ^{1}H NMR spectra of CP_3 and CP_3-$MPEG_{12}$ in $CDCl_3$.

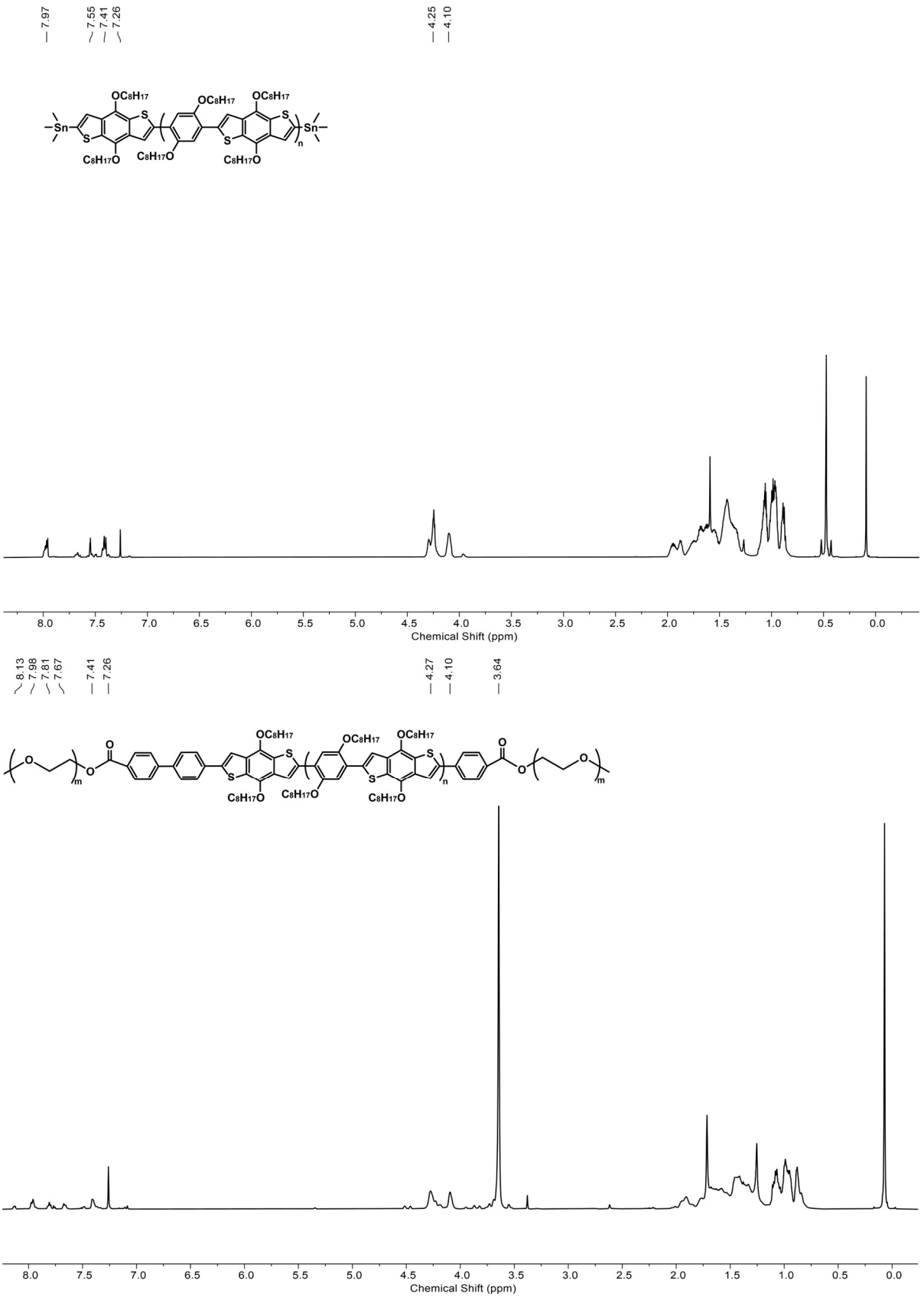

Figure S25. The ^{1}H NMR spectra of CP_4 and CP_4-$MPEG_{12}$ in $CDCl_3$.

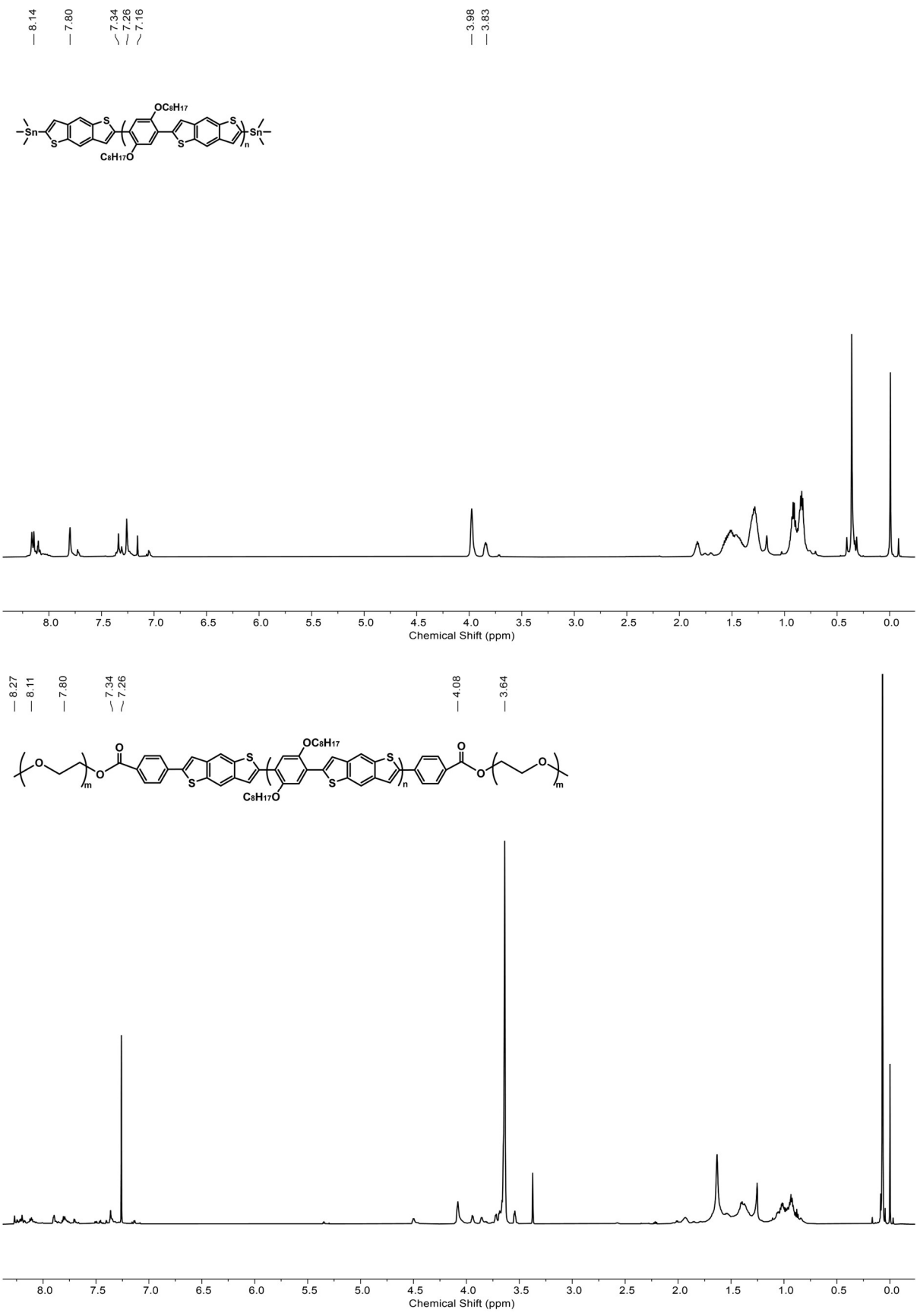

Figure S26. The ^{1}H NMR spectra of CP_5 and CP_5-$MPEG_{12}$ in $CDCl_3$.

References

1. B. N. Norris, T. Pan and T. Y. Meyer, *Organ. Lett.*, 2010, **12**, 5514-5517.
2. R. H. Pawle, A. Agarwal, S. Malveira, Z. C. Smith and S. W. Thomas, III, *Macromolecules*, 2014, **47**, 2250-2256.
3. C. Y. Mei, L. Liang, F. G. Zhao, J. T. Wang, L. F. Yu, Y. X. Li and W. S. Li, *Macromolecules*, 2013, **46**, 7920-7931.
4. P. F. Gao, Y. Zhang, J. L. Ni, B. Zheng, L. Y. Wang, H. Y. Fu and L. J. Huo, *Polymer*, 2022, **246**.
5. Y. Wu, J. Wang, Y. Zhu, X. Yu, Z. Shang, Y. Ding and A. Hu, *Chem. Commun.*, 2021, **57**, 4146-4149.
6. S. Deng, J. Zhi, X. Zhang, Q. Wu, Y. Ding and A. Hu, *Angew. Chem. Inter. Ed.*, 2014, **53**, 14144-14148.
7. S. Kobayashi, K. Fujiwara, D. H. Jiang, T. Yamamoto, K. Tajima, Y. Yamamoto, T. Isono and T. Satoh, *Polym. Chem.*, 2020, **11**, 6832-6839.
8. D. Zhao, J. Feng, Q. Huo, N. Melosh, G. H. Fredrickson, B. F. Chmelka and G. D. Stucky, *Science*, 1998, **279**, 548-552.
9. F. Ziegler, J. Teske, I. Elser, M. Dyballa, W. Frey, H. Kraus, N. Hansen, J. Rybka, U. Tallarek and M. R. Buchmeiser, *J. Am. Chem. Soc.*, 2019, **141**, 19014-19022.
10. J. D. Webb, T. Seki, J. F. Goldston, M. Pruski and C. M. Crudden, *Micropor. Mesopor. Mater.*, 2015, **203**, 123-131.
11. C. J. O'Brien, E. A. B. Kantchev, C. Valente, N. Hadei, G. A. Chass, A. Lough, A. C. Hopkinson and M. G. Organ, *Chem.-Eur. J.*, 2006, **12**, 4743-4748.